Received: 20 June 2023 | Revised: 24 April 2024 | Accepted: 2 May 2024

DOI: 10.1002/rra.4309

RESEARCH ARTICLE

WILEY

Observation of high sediment concentrations entrained in jumble river ice

Christopher D. Arp[1] | Allen C. Bondurant[1] | Sarah Clement[2] | Emily Eidam[3] | Ted Langhorst[4] | Tamlin M. Pavelsky[5] | Julianne Davis[5] | Katie V. Spellman[2]

[1]Water and Environmental Research Center, University of Alaska Fairbanks, Fairbanks, Alaska, USA

[2]International Arctic Research Center, University of Alaska Fairbanks, Fairbanks, Alaska, USA

[3]Department of Earth, Ocean, and Atmospheric Sciences, Oregon State University, Corvallis, Oregon, USA

[4]Department of Civil and Environmental Engineering, University of Massachusetts Amherst, Amherst, Massachusetts, USA

[5]Department of Earth, Marine, and Environmental Sciences, University of North Carolina, Chapel Hill, North Carolina, USA

Correspondence
Christopher D. Arp, Water and Environmental Research Center, University of Alaska Fairbanks, Fairbanks, AK 99775, USA.
Email: cdarp@alaska.edu

Funding information
National Science Foundation, Grant/Award Numbers: 2153778, 1836523

Abstract

Ice formation is generally considered to exclude many particles and most solutes and thus be relatively pure compared to ambient waters. Because river ice forms by a combination of thermal and mechanical processes, some level of sediment entrainment in the ice column is likely, though reports of sediment in river ice are limited. We observed high and sporadic levels of silt and sand in ice of the Kuskokwim and Tanana rivers (Alaska, the United States) during routine field studies. These observations led us to make a more comprehensive survey of sediment entrainment in river ice of the Kuskokwim and Yukon rivers and several of their tributaries. We collected and subsampled 48 ice cores from 19 different river locations in March 2023, which included concurrent measurements of water turbidity, velocity, and depth. Approximately 60% of cores contained detectable levels of sediment, averaging 438 mg/L with median concentrations exceeding 1000 mg/L in three cores from the Yukon and Kuskokwim main stems. Many cores had even higher concentrations at certain intervals, with seven cores having subsamples exceeding 2000 mg/L; these were often located in the middle or lower portion of the ice column. Jumble ice, formed mechanically by frazil-pan jamming during freeze-up, was generally the best predictor of higher sediment entrainment, and these locations often had higher under-ice velocities and depths. Our observation of high and widespread sediment entrainment in northern river ice, particularly in jumble-ice fields, may have implications for sediment transport regimes, ice strength and transportation safety, and how rivers break up in the springtime.

KEYWORDS
Alaska, freeze-up processes, northern rivers, river ice, sediment

1 | INTRODUCTION

Principles of fluvial sediment transport suggest that sediment discharge increases with water discharge (Knighton, 1998; Leopold et al., 1964) and that northern alluvial rivers can have both supply-limited and transport-limited sediment regimes (Beltaos & Burrell, 2021; Turcotte et al., 2011). Thus in cold-region rivers, the expectation is that the majority of sediment is transported during open-water periods fed by snowmelt runoff, glacier melt, and rainstorms in the late spring to early fall when river discharge is variably

high and watersheds and channels are most susceptible to erosion (Dornblaser & Striegl, 2009; Kämäri et al., 2015; McNamara & Kane, 2009). Declining winter flows and frozen, snow-covered uplands should then correspond to increasingly clear-water discharge in ice-covered rivers until spring breakup (Beltaos & Burrell, 2021; Turcotte et al., 2011). Quantitative models of river sediment flux reflect this general conceptual model, perhaps because the vast majority of sediment-load observations come from summer open-water periods (Chikita et al., 2002; Dornblaser & Striegl, 2009; Syvitski, 2002; Syvitski et al., 2005). Thus, when we encountered significant sediment entrained in ice during winter field studies on a few northern rivers (Figure 1), we became curious as to how these observations complemented or contradicted the paradigm that little sediment moves during the ice-covered season.

Similar observations of high sediment entrainment in ice have been made by other scientists including from the Laramie River in Wyoming (the United States) (Kempema & Ettema, 2011), several regulated rivers in northcentral Canada (Kalke et al., 2017), and the Tanana River in Alaska (Lawson et al., 1986; Osterkamp, 1977). Ice rafting of sediment from mobilized anchor ice and more general frazil-ice entrainment of sediment have been suggested as important transport processes during river freeze-up (Ettema & Daly, 2004; Kempema & Ettema, 2011; Turcotte et al., 2011). Continued frazil-ice generation in open-water leads, which can produce hanging dams (thick under-ice frazil deposits), may also cause locally enhanced bed scour, mobilized sediment, and downstream storage in ice-pan jamming fronts and jumble-ice covers (Ettema & Daly, 2004; Turcotte et al., 2011). More abundant documentation of sediment ice-entrainment comes from near-shore marine and large lake environments where pancake ice and wave action are known to erode, raft, and entrain large amounts of sediment of various caliber in cold regions (Kempema et al., 2001; Reimnitz et al., 1987). These studies demonstrate multiple processes and environments where sediment entrainment in ice is significant, as well as emphasizing that these sediment-ice processes and patterns (1) remain poorly understood, (2) generally are neglected in fluvial sediment transport concepts and models (Burrell et al., 2021), and (3) cause largely unknown environmental and engineering impacts (Ettema & Daly, 2004; Kempema & Ettema, 2011).

Thus to better understand how widespread ice sediment-entrainment is in northern rivers, we undertook an initial inventory of late winter ice quality with respect to sediment in the Kuskokwim and Yukon rivers and their tributaries in interior and western Alaska. In addition to sampling a range of river sizes and hydrogeomorphic conditions, we also systematically collected ice cores from locations with varying freeze-up timing and potentially differing ice consolidation processes. Our goal in this study was to begin documenting where and how much sediment ice-entrainment occurs in a set of northern rivers in order to advance future models and monitoring strategies of sediment transport in ice-affected rivers.

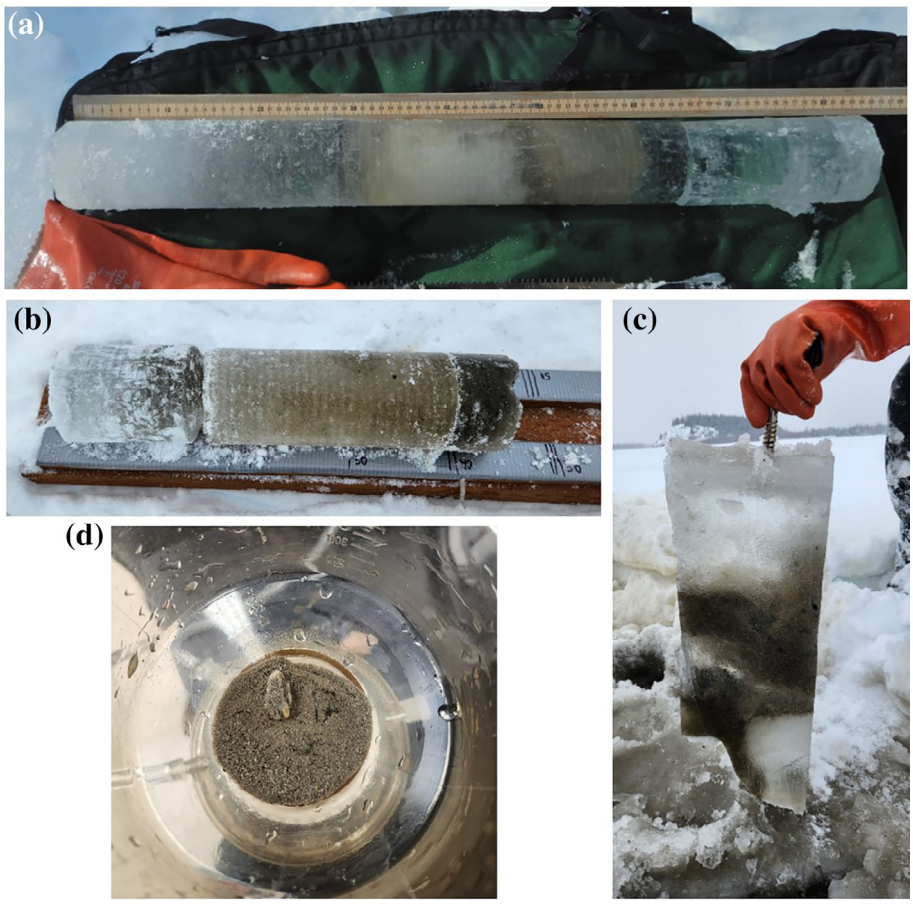

FIGURE 1 Example photographs from early observations made of high sediment concentrations in ice from the Kuskokwim River in 2022 (a) and the Tanana River in 2023 (b–d). Image (c) is an ice block cut adjacent to the same location as image (b) collected in a jumble-ice field. Image (d) shows the sediment collected on a filter from a ~5 cm thick subsample with coarse sand and larger gravel-sized clast. [Color figure can be viewed at wileyonlinelibrary.com]

2 | METHODS

All sampling for this study was conducted on the Yukon and Kuskokwim rivers, the two largest rivers in Alaska, and their tributaries (Figure 2, Table 1) in the mid- to late-winters of 2022 and 2023. Initial observations were made on the Kuskokwim River in March 2022 during ice and snow monitoring to inform ice-jam flood forecasting (Figure 1a). More targeted studies were conducted on the Tanana River in mid-winter of 2023, in part to develop and test methods and characterize how sediment varied with ice-column stratigraphy (Figure 3) and among varying positions on the river-ice surface (Table 2). Based on this work, we selected 23 sites on nine river reaches in western Alaska for more extensive ice coring and sediment sampling in March 2023 (Figure 2a). River reaches were selected opportunistically to overlap with a known and safe travel route between the communities of McGrath, Shageluk, and Galena along the Iditarod Trail. Exact locations for ice coring were based on position relative to individual late-freezing open-water zones (OWZs) identified from late November 2022 optical imagery (Landsat 8 or Sentinel-2) (Figure 2c). The heads of OWZs were assumed to freeze last, typically in December or later, tails of OWZ were assumed to freeze earlier, and locations adjacent to OWZ were known to have ice cover at the time of image acquisition and thus froze earliest. By selecting sampling locations relative to known OWZ, we were able to differentiate and make general inferences about ice formation processes that were consistent among sites, river reaches, and river systems. Because the few previous inventories of sediment entrainment in river ice are limited to single river reaches without hydrogeomorphic stratification of sampling locations (Ettema & Daly, 2004; Lawson et al., 1986), we did not have an a priori specific hypotheses about how ice sediment content might vary among these positions, though we did anticipate differences might be related to freeze-up timing and mechanism, as we later discovered.

For the extensive inventory part of this study, all sites were visited by snow machine between 11 and 23 March 2023 and we were typically able to sample one to three locations per day among travel, other field studies, and community science-outreach activities. As a standard safety procedure, our team of three always navigated to early freezing zones (EFZ) first and measured ice thickness to ensure conditions were safe in the area where ice had been growing the longest. Next, while two team members began sampling and data collection, one person drove a snow machine with no sled to the middle freezing zone (MFZ) to check ice thickness while being spotted by the other team members. This was then repeated at the late freezing zone (LFZ) before returning to the EFZ to complete measurements. In practice, overflow was as much a concern as thin ice, but fortunately we found no ice thinner than 40 cm (>25 cm is considered safe for snow machine travel), and most overflow encountered did not limit our travel. Of the 23 sites originally selected, we were able to completely sample 17. Two were only partly sampled due to open water still being present at MFZ and LFZ locations. At one OWZ, the entire area had open water and was obviously not sampled, and three were in locations where overflow made travel too hazardous.

At each site associated with an OWZ, we collected 7.3-cm diameter ice-cores from each EFZ, MFZ, and LFZ location with a Kovacs (Mark III) 1-m core-barrel driven with a rechargeable drill. Cores were photographed, stratigraphic notes collected, and an increment of median and maximum sediment concentration was identified visually, separated with a hand saw, and stored in a zip-lock bag. We typically collected ~5 cm (~500 mL) subsamples for analysis of sediment and stored these samples in a padded container to prevent damage and sample loss during snow machine travel. For the initial pilot studies conducted on the Kuskokwim River in 2022 and Tanana River in 2023, ice cores were subsampled at even increments (5–10 subsamples per core depending on total length) to provide a more accurate estimate of total ice-column sediment and guide our sampling strategy for collecting cores and subsampling in remote locations where time and sample storage were more limited. At the same core-barrel auger holes at each of three locations per OWZ, we placed two OpenOBS optical backscatter (OBS) turbidity sensors (Eidam et al., 2022; Langhorst et al., 2023) at offset increments at approximately mid-point in the water column to log data at 10-s intervals for at least 1 min and typically closer to 5 min. Next, velocity profiles were recorded for three 40-s intervals using an acoustic doppler current profiler (ADCP, RDI Teledyne Streampro WaterMode 12), which were later summarized according to profile mean and maximum velocities, identify depths of maximum velocity, and associated variance for each statistic. Aerial drone photos were collected at most sites when weather conditions allowed, surface conditions were noted (e.g., smooth vs. jumble, black-ice vs. snow-ice, and the presence of overflow), and several other standard field measurements were collected including ice thickness, snow depth, and water temperature and conductivity profiles for other studies. These data are not reported here, but can be accessed at the Arctic Data Center (Arp et al., 2024).

Ice samples were melted at room temperature, then passed through a 47-mm diameter Type A/C glass fiber filter (0.7 micron pore-size) with a hand vacuum pump to collect sediment. Sample filters processed at field camps or remote communities were then folded in half and placed in a foil envelope. In the lab, filters were dried at 100°C for 4 h and then weighed using a micro-balance (Ohaus Scout Pro) to 0.01 g. Typical detection limits for a 500 mL sample were determined to be 20 mg/L. For all statistical summations and graphical analysis, samples below this detection limit were assigned a median value of 10 mg/L. Grain-size distributions were only classified qualitatively (visually), and no separation of organic from mineral fractions was completed. All ice sediment concentrations (ISC) reported in Table 2 are from multi-core distributions of median ice-sediment concentrations (median ISC) averaged per river reach and do not include single-core samples of visually determined maximum ice-sediment concentrations (max ISC), which were collected and quantified for many cores.

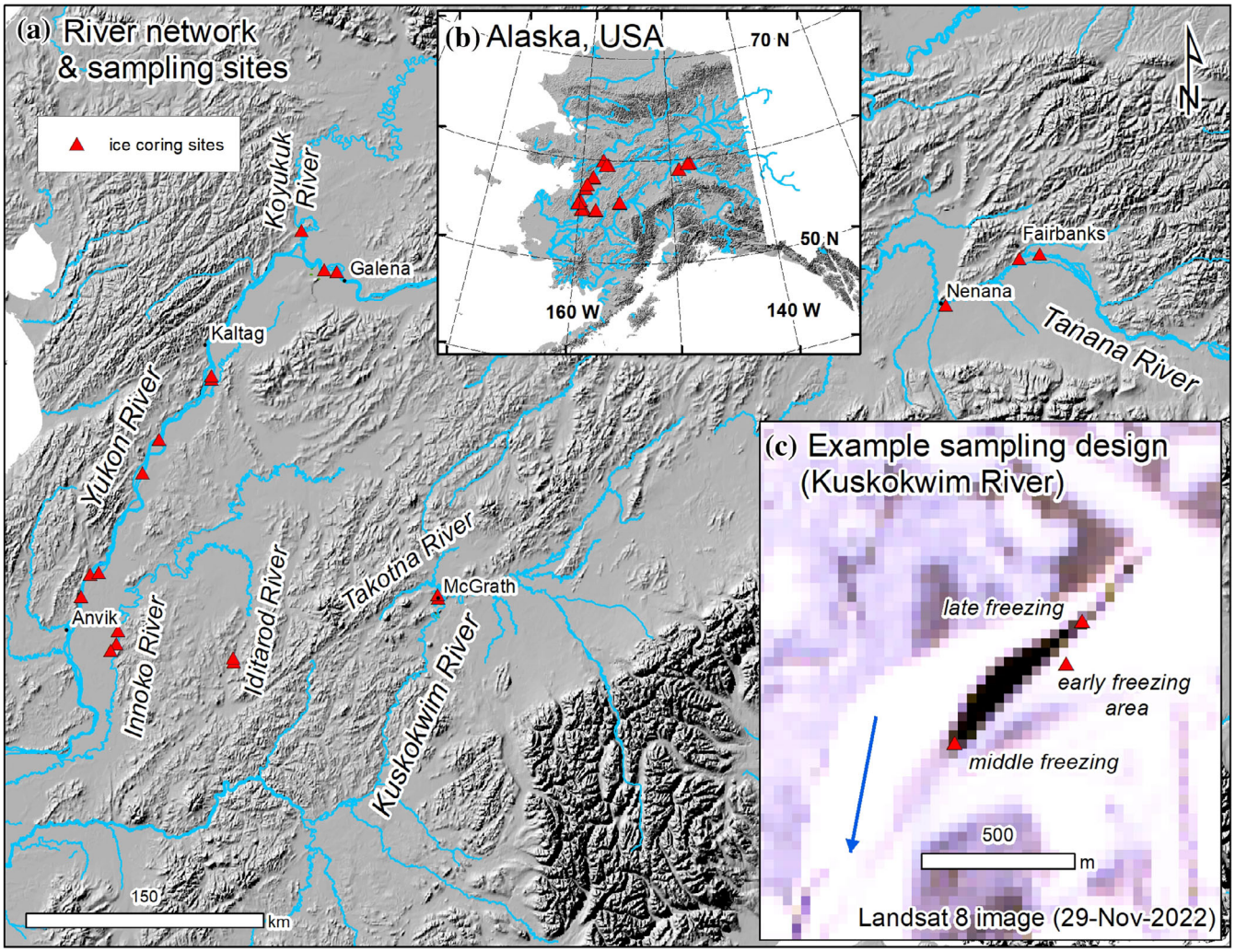

FIGURE 2 Drainage and topographic map of western to interior Alaska showing locations of study reaches and ice core sampling (a) within Alaska, the United States (b). Panel (c) shows an example of our sampling location design within river reaches where exact locations were selected based on late November optical satellite imagery used to identify late freezing areas on most rivers. [Color figure can be viewed at wileyonlinelibrary.com]

TABLE 1 Study reach characteristics.

River	Adjacent communities	Width (m)	Slope (%)	Sinuosity	Channel form
Tanana	Nenana	360	0.063	1.2	Meandering
Tanana	Fairbanks (downstream)	280	0.067	1.1	Anastomosing
Tanana	Fairbanks (upstream)	430	0.026	1.3	Braided
Kuskokwim	McGrath	270	0.028	2.4	Meandering
Takotna	McGrath	90	0.031	3.2	Meandering
Yukon	Galena, Koyukuk	1330	0.001	1.2	Anastomosing
Koyukuk	Koyukuk	350	0.004	1.8	Meandering
Yukon	Kaltag, Nulato	1910	0.001	1.1	Anastomosing
Yukon	Eagle Island	2010	0.001	1.1	Anastomosing
Yukon	Grayling, Anvik	1390	0.002	1.1	Anastomosing
Innoko	Shageluk	230	0.037	1.4	Meandering
Iditarod	Iditarod City	50	0.066	1.7	Meandering

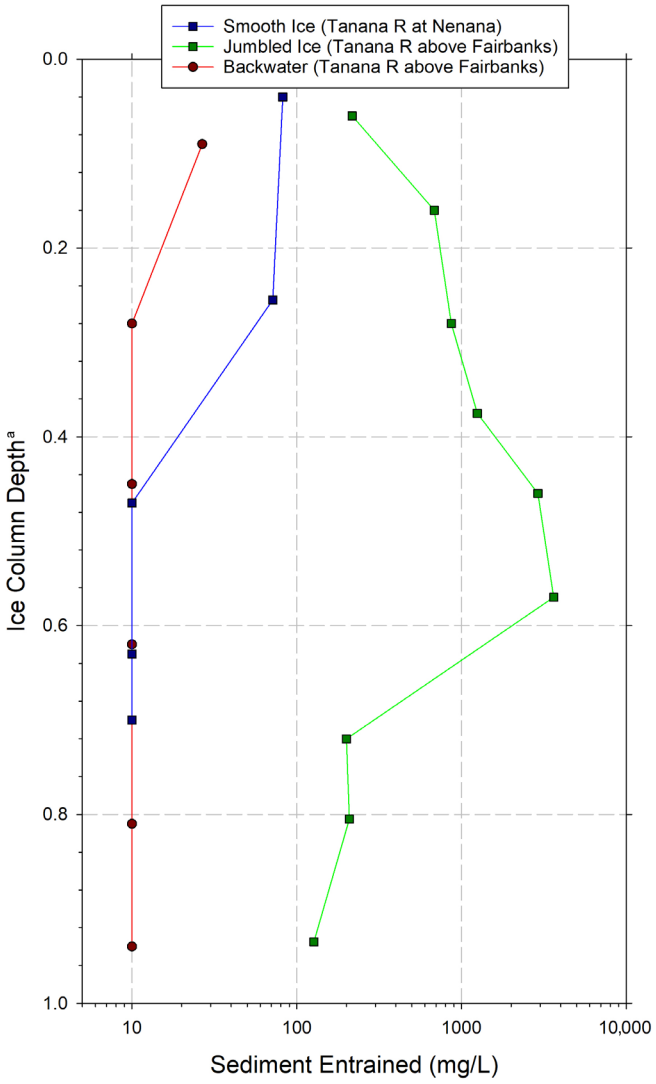

FIGURE 3 Down-core variation in sediment concentrations from ~5 cm subsamples collected at ~10–20 cm intervals depending on total core length. [a]Subsample location relative to total core length. [Color figure can be viewed at wileyonlinelibrary.com]

3 | RESULTS

Sediment was much more common in the ice of larger rivers in this study (Yukon, Tanana, and Kuskokwim rivers), with 81% of cores having detectable sediment concentrations, compared to smaller tributaries where only 35% of cores had detectable concentrations (Tables 1 and 2). The highest sediment concentrations we discovered were on a constricted reach with a prominent jumble-ice field on the Tanana River downstream of Fairbanks, where we subsampled the entire core and found an average concentration of almost 12 g/L and maximum subsample concentration exceeding 50 g/L (Table 2, Figure 1b–d). Another sampling location on the Tanana River, also located in a jumble-ice field and fully subsampled, had average sediment concentration of 1.2 g/L and maximum concentrations exceeding 5 g/L. Locations on the Kuskokwim and Yukon rivers with higher concentrations were also associated with zones of jumble ice (Figure 4b). For locations on smaller rivers with detectable sediment, concentrations were much lower, averaging 72 mg/L from median ISCs. A backwater area of the Tanana River that we sampled as a reference had detectable sediment in only one of six subsample increments collected over the full core and the detectable increment was near the surface (Figure 3, Table 2).

For ice cores where we collected two subsamples, targeting median and maximum concentrations based on visual inspections, maximum sediment concentrations ranged from nearly equivalent to the median subsample values up to several orders of magnitude higher than the median subsample values, most notably on the Iditarod and Yukon rivers (Figure 5). Down-core locations of maximum concentrations sampled generally occurred in the lower portions of the core and often near the base (Table 2, Figure 6). In several Tanana River cores that were subsampled evenly, sediment concentrations were much higher in the middle of the core in jumble ice and only detectable near the surface for cores collected in smooth river and backwater ice (Figure 3).

Measuring late winter water-column turbidity was often limited by sub-ice frazil accumulations, but where possible averaged about 100 NTU (Table 2) and were somewhat higher in the larger rivers we sampled (Figure 7). Sub-ice water velocities averaged 0.3 m/s and ranged from near zero (location sampled on the Yukon River) to almost 1 m/s (location sampled on the Kuskokwim River). Water depths at sampling locations averaged 3.2 m and ranged from 0.9 m at a location on the Koyukuk River to >7 m (limits of ADCP transducer) at multiple river locations. We converted these data to specific discharge (velocity × depth) to compare with sediment-ice concentrations, which show generally higher sediment with deeper and higher velocity river locations (Figure 4). Later freeze-up timing classifications (MFZ and LFZ) tended to have higher specific discharge, but levels of sediment in ice were highly varied for locations with specific discharge >1 m^2/s (Figure 4a). Surface conditions classified as jumble or smooth were not necessarily related to specific discharge, though concentrations of sediment in jumble ice averaged 748 mg/L compared to 36 mg/L in smooth ice (Figure 4b). Our ability to classify zones of jumble ice was often limited by areal extent and surface roughness relative to snow depth and overflow refreeze, such that some locations classified as smooth may have been formed by frazil-pan/pancake ice jamming and this was not always easily identified by inspection of core stratigraphy (Figures 1 and 6). Where jumble-ice fields were evident on the surface according to irregularities in the snowpack and particularly where ice pans were sticking above the snow surface, high sediment concentrations were often visually apparent in protruding ice slabs (Figure 8).

4 | DISCUSSION

River freeze-up typically begins once air temperature falls below freezing and particularly during clear, cold (<−20°C) nights that promote supercooling of water and frazil-ice formation (Ashton, 2011;

TABLE 2 Ice sediment sampling results reported by river reach (turbidity was measured in the middle of the water column below each core points).

River reach	Month-year	Z_{ice} (cm)	Turbidity (NTU)	No. of cores	Ice sediment concentration (median ISC) (mg/L)			Max ISC location in column	Dominant sediment type
					Mean	Max	Min		
Kuskokwim at McGrath	Feb-22	84	nd	7	471	1750	bd	Middle–bottom	Silt
Kuskokwim at McGrath	Mar-23	61	85.2	6	388	1097	bd	Middle–bottom	Silt
Tanana below Fairbanks	Jan-23	45	nd	3	11,869	24,133	800	Middle–bottom	Sand
Tanana at Fairbanks	Feb-23	92	nd	2[a]	869	5450	bd	Middle	Sand
Tanana at Fairbanks[b]	Feb-23	68	nd	1[a]	4	27	bd	Surface	Silt/organic
Tanana at Nenana	Feb-23	59	nd	2[a]	37	133	bd	Surface	Silt/organic
Tokatona above McGrath	Mar-23	62	83.1	6	8	25	bd	Surface–middle	Silt/organic
Yukon near Grayling	Mar-23	68	157.5	4	186	714	bd	Middle	Silt
Yukon near Eagle Island	Mar-23	73	97.0	6	521	857	86	Varied	Silt
Yukon near Kaltag	Mar-23	74	nd	6	854	3333	bd	Middle–bottom	Silt
Yukon near Galena	Mar-23	74	nd	4	119	314	34	Middle–bottom	Silt
Koyukuk above Koyukuk	Mar-23	63	nd	3	43	100	bd	Bottom	Silt/organic
Innoko near Shageluk	Mar-23	56	102.6	7	40	211	bd	Surface-bottom	Silt/organic
Iditarod near Iditarod City	Mar-23	50	nd	6	bd	bd	bd	Middle	Silt/organic

Abbreviation: bd, below detection of 20 mg/L; nd, data not collected; ISC, ice sediment concentrations; Z_{ice}, ice thickness.
[a]Multiple subsamples collected through the entire core.
[b]River backwater area with lentic properties.

Osterkamp & Gosink, 1983). Border ice grows thermally by heat loss in low velocity margins and backwaters, while frazil-ice production and transport in turbulent water leads to a range of thermo-mechanical processes eventually forming a contiguous ice cover in northern rivers with long cold winters (Burrell et al., 2021). The formation of anchor ice is most evident in smaller, steeper gradient streams where it is known to build upon and eventually raft large gravel and even cobble in some instances (Ettema & Daly, 2004; Kempema & Ettema, 2011). Anchor ice can also form in larger rivers on coarse sediment below turbulent, frazil-ice production zones with perhaps lower limits on buoyancy and rafting (Turcotte et al., 2011), though Kempema and Ettema (2011) suggest that anchor ice masses forming on fine sediment in larger rivers can be buried under migrating bedforms before initial rafting. Accumulated frazil-floc eventually forms frazil-pans or pancake-ice, which grow with continued interaction with border ice and other frazil pans during downstream transport. During variable water levels, these frazil pans may also interact with fine sediment as pans lodge on bars and are refloated downstream. Though river discharge is typically declining during the freeze-up period, water levels often sporadically increase as channel geometry shrinks and roughness increases during stages of ice-cover formation (Turcotte et al., 2011). Thus, there are multiple opportunities for sediment to be entrained and concentrated in ice pans before they eventually arrest or jam at accumulation fronts that build upstream. For larger rivers in zones of high or variable velocity, jumble-ice fields formed by pancake-ice jamming can be extensive (tens of kilometer) and it is in these types of areas on the Tanana, Yukon, and Kuskokwim rivers where we generally found high and heterogeneous deposits of silt and sand in ice.

Interestingly, but perhaps not surprisingly, accumulations of sediment were generally highest in middle to lower portions of the ice cores and blocks we sampled. The theoretical maximum sediment load ice can transport is 122 g/L before losing its buoyancy (Ettema & Daly, 2004), and it follows that upon jamming, portions of ice pans with higher sediment concentrations would preferentially orient lower in the water column. Once ice pans are in place, whether lying flat on

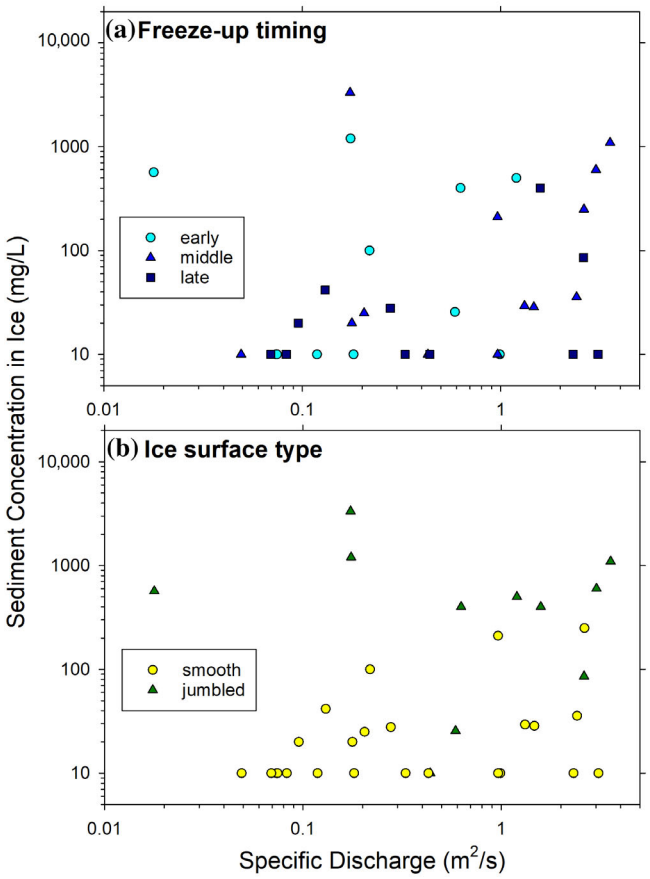

FIGURE 4 Comparison of sediment ice concentrations (median ice sediment concentrations) with specific discharge (product of average water column velocity and water depth) for each core location grouped by relative freeze-up timing (see Figure 2c) (a) and ice surface conditions observed during sampling in March 2023 (b). [Color figure can be viewed at wileyonlinelibrary.com]

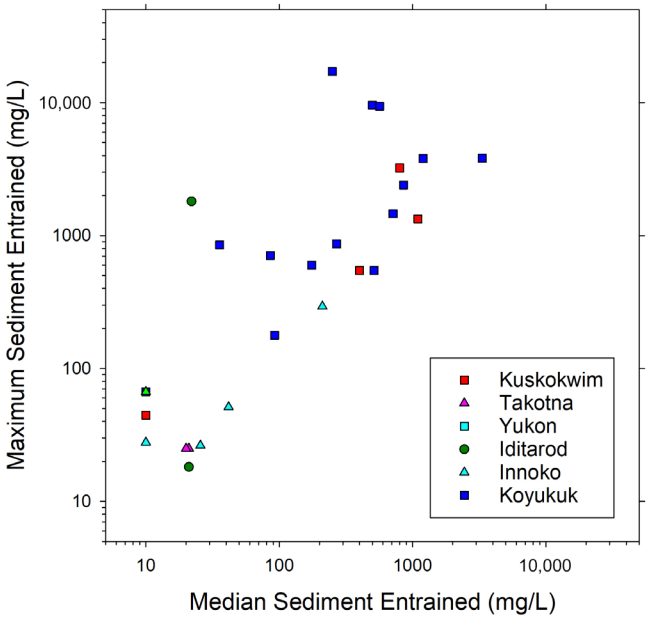

FIGURE 5 Comparison of median sediment concentrations (median ice sediment concentrations [ISC]) to maximum sediment concentrations (maximum ISC) (per core) averaged across study rivers. [Color figure can be viewed at wileyonlinelibrary.com]

the water surface or thrust more vertically during jamming, interstitial space within the arrested ice-pan matrix rapidly fills in with frazil- and congelation-ice and additional thermal-ice and frazil-accumulations thicken the ice cover (Burrell et al., 2021). If anchor-ice rafting and frazil-pan transport are the major processes in which sediment is entrained in the ice cover, we would thus expect deposits to be highly variable both horizontally and vertically perhaps at the scale of individual pans (10 cm to 10 m in diameter) and be most pronounced in jumble-ice fields as we observed. Although not specifically observed in this study, we also suspect that wind-blown silt and sand deposited on river ice can be locally or regionally important in many northern rivers, and if present, such accumulations would be found on the ice surface or entrained in snow ice (refrozen overflow).

Based on experience traveling hundreds of kilometer of river over several years, we know that jumble-ice fields can be extensive, extending bank-to-bank and often many kilometers in distance downstream. We are not aware of any studies rigorously documenting extents of jumble-ice cover in Alaska or other rivers using remote sensing or field surveys, though observations of rough jumble-ice cover are common from river travelers including snowmachiners, sled-dog mushers, and community groups constructing and maintaining ice roads. Observations from the winter of 2022–2023 suggest that jumble-ice fields on the Yukon River were rougher and more expansive than normal, with thicker deposits of unconsolidated frazil underlying solid ice cover (personal communications M. Schellekens, K. Bodony, and students and teachers at Eagle Community School). Thus, ice samples collected for this study may have held higher sediment concentrations than are typical of most years. Anecdotal evidence suggests that a late freeze-up coupled with several spates of abnormally cold weather and snowfall may have helped produce river conditions conducive to multiple episodes of frazil- and anchor-ice production and extended ice-pan transport before jamming and ice-cover consolidation.

In this study we selected coring locations based on ice-cover conditions observed in late November 2022 from optical satellite imagery (Landsat 8 or Sentinel-2), which correspond to freeze-up timing and likely freeze-up process—though process is only inferred from position relative to open leads and might vary by river size or other hydrogeomorphic attributes. Generally, we expected EFZs to be a combination of border ice and lodged pancake-ice, whereas open-lead tails (MFZs) were most likely upstream accumulating frazil-ice and jammed pancake-ice. While open-lead heads (LFZs) may have been just below upstream freeze-up jams and more likely to have formed thermally with less frazil contributions. During field visits, we found no consistent and distinct patterns in ice thickness nor surface conditions among these river positions relative to OWZs, though the outlines of open leads were often visible from drone imagery. Ice sediment concentrations, however, were distinctly higher in EFZs and MFZs, 430 and 309 mg/L, respectively, compared to LFZs averaging

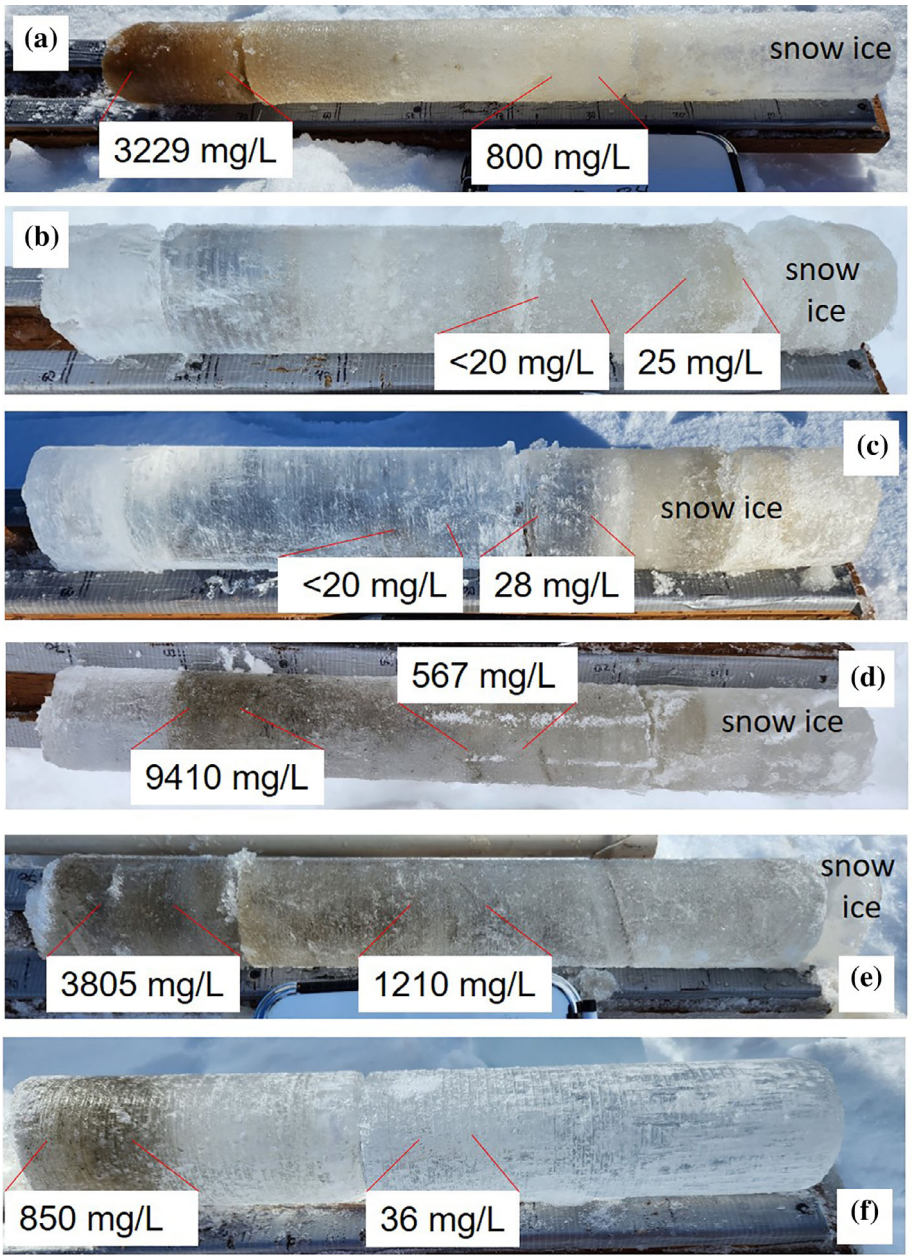

FIGURE 6 Example ice core photographs from the Kuskokwim (a), Takotna (b), Innoko (c), and Yukon (d–f) rivers. Each core was subsampled at a location that appeared to have an average sediment concentration and a maximum sediment concentration. Locations of higher sediment generally were found lower in each ice core, though many had no distinct band with high sediment. [Color figure can be viewed at wileyonlinelibrary.com]

80 mg/L of ice-entrained sediment. These results do help confirm the important role of frazil ice in mobilizing and transporting sediment (Ettema & Daly, 2004; Kalke et al., 2017; Turcotte et al., 2011), as we suspect LFZs are least likely to be influenced by frazil-ice accumulation. Additionally, an ice core collected and fully subsampled from a backwater zone of the Tanana River, where we expected only congelation (thermal) ice growth, only had detectable sediment in the near-surface increment (Figure 3), providing further evidence of the need for turbulent flow and frazil ice to entrain sediment in the full ice column. Future sampling used to extrapolate to reach-scale sediment storage in ice may look to stratify ice formation features more completely using a combination of optical imagery, in which late November is typically the latest imagery available at this latitude, and mid-winter radar imagery (e.g., Sentinel-1 synthetic aperture radar) to detect variation in surface and sub-ice roughness (Engram et al., 2024).

Implications of sediment-entrainment in ice beyond its role in sediment transport may include impacts on ice strength regarding ice-road construction and ice degradation during breakup. Literature pertaining to ice strength suggests black- or thermal-ice has greater load bearing capacity than white- or snow-ice, and freshwater ice has greater load bearing capacity than sea ice (Masterson, 2009), suggesting that ice strength may be reduced with higher sediment content. Perhaps the more salient consideration is how the strength of jumble ice compares to smooth thermal-ice, as our study shows these ice types are strongly related to ice quality with respect to sediment. We have not found distinct consideration of jumble ice treated in research on ice strength and ice road construction, though conventional

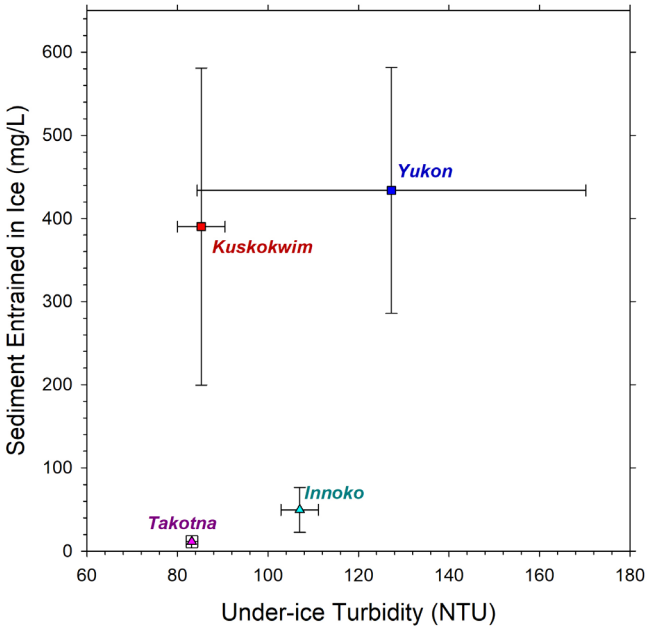

FIGURE 7 Comparison of mean under-ice turbidity recording in March 2023 for four study rivers compared to median sediment ice concentrations (median ice sediment concentrations, bars are standard errors). [Color figure can be viewed at wileyonlinelibrary.com]

wisdom suggests that jumble ice may provide a safer travel route if the traveler can bear the bumps (Schneider et al., 2015).

Regarding the role of ice-sediment content in river breakup, there is little doubt that dark impurities in ice such as sediment will cause more rapid melt and degradation compared to clear- or black-ice. Many approaches to ice-jam mitigation have been tested over the years in the United States and Canada including the practice of dusting ice with fine sediment in locations of potential ice-jams to accelerate melt, though the efficacy of this practice appears limited (Belore et al., 1990; White & Kay, 1997). The position and heterogeneity of sediment concentrations in river ice may also factor into its impact on melt rate and eventual disintegration. Our sampling suggests that sediment concentrations are often higher near the middle or base of the ice column, such that much of this sediment may be released during early melting driven by increasing flows and water temperature. In the case of mechanical breakup events where ice-covers are fractured by rising water levels and can result in ice jams and flooding, sediment in ice may weaken the ice cover to create smaller and less stable fracture pans with shorter downstream travel distances before complete melt and disintegration.

Understanding how ice-entrained sediment impacts breakup in terms of process and timing may also be relevant to the role of ice in sediment transport, as it is well understood that the balance of sediment supply and transport capacity are changing dramatically during

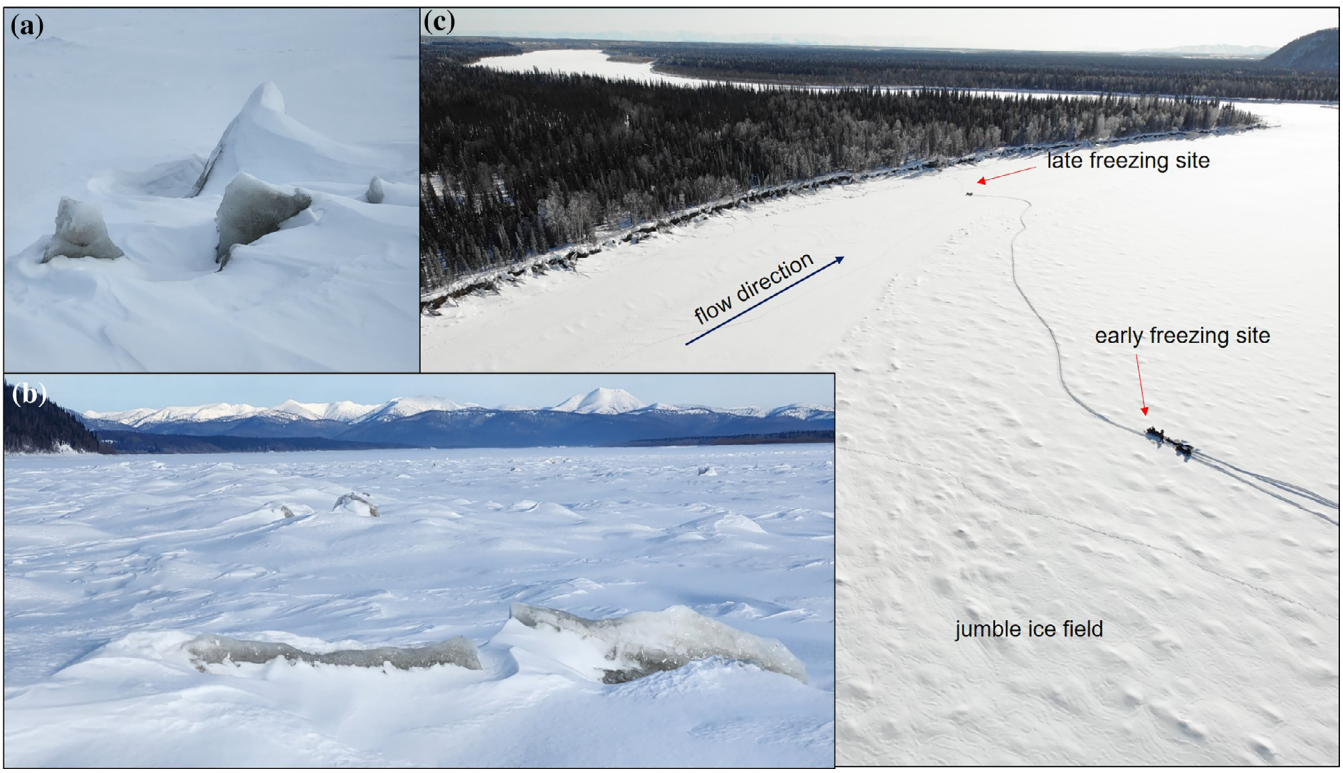

FIGURE 8 View of sediment-laden jumble ice on the Yukon River (a, b) and a jumble-ice field associated with sampling locations on the Kuskokwim River (c). Two of three sampling locations associated with a freeze-up timing sequence are shown in panel (c) and snow machines and sleds in the photo can be used for scale. In late winter of most years, jumble ice is often common on larger rivers, but hard to see depending on snow conditions. [Color figure can be viewed at wileyonlinelibrary.com]

the river breakup period (Beltaos & Burrell, 2021). Releasing ice-stored sediment back into the water column on the rising limb of the snowmelt hydrograph of large rivers may allow long and effective downstream transport. In cases of ice-jam backwater-flooding and ice-jam release waves (javes), abundant sediment may already be mobilized from watershed runoff, high and unsteady river discharge, and ice disturbance of beds and banks, such that additional contributions from the melting ice column may fall into an already over-supplied sediment transport environment. Future research that is able to quantify river sediment flux during the various stages of breakup using novel sensor deployment (i.e., OBS sensors, Eidam et al., 2022; Langhorst et al., 2023) may help resolve how important ice-column sediment release is to overall river sediment budgets.

5 | CONCLUSIONS

Our results from sampling 11 river reaches of varying size and character over two winters in western and interior Alaska suggest widespread, variable, and often high levels of sediment entrainment in ice. The highest concentrations observed occurred on the larger channels of the Yukon, Tanana, and Kuskokwim rivers in zones of jumble-ice accumulation compared to smaller rivers where smooth ice was more prevalent. Correspondence of higher sediment in jumble-ice formed by ice-pan accumulation (i.e., juxtapositioning) fronts, along with finding higher sediment concentrations in the middle or lower portion of ice cores, suggests that frazil-ice formation, transport, and evolution to large ice pans play an important role in sediment mobilization and winter storage. This winter sediment transport mechanisms appear to be in contrast to observations and models focused on summer open-water periods where the majority of sediment is supplied, mobilized, and transported.

This research builds on a limited set of studies also documenting patterns and processes of ice sediment-entrainment in northern rivers including on the Tanana River in Alaska where a portion of this study also took place. Perhaps of great relevance in the literature review presented by Kempema and Ettema (2011), it is noted that in *Principles of Geology* by Lyell (1868), the importance of ice in river sediment transport is specifically mentioned, yet this process has since been routinely neglected in most fluvial geomorphology texts (Knighton, 1998; Leopold et al., 1964). Thus, it is incumbent on our research team and others studying ice-affected rivers to consider and build upon this work presented here and in other studies to better understand and communicate the role of river ice in sediment transport and other fundamental fluvial processes. Considering the dramatic changes ice-affected rivers are currently experiencing (Yang et al., 2020), understanding the role of ice in sediment transport is even more urgent.

ACKNOWLEDGMENTS

This research was supported by funding from the National Science Foundation through Sediment and Ice Learning on the Tanana (#2153778, #1836523). We thank students, teachers, and local scientists in Fairbanks, Nenana, McGrath, Shageluk, and Galena for support of this research through fieldwork and logistical assistance. We thank two anonymous reviewers for a pointed and helpful evaluation of this paper.

DATA AVAILABILITY STATEMENT

The data that support the findings of this study are openly available in Arctic Data Center at 10.18739/A2086372J.

ORCID

Christopher D. Arp https://orcid.org/0000-0002-6485-6225

REFERENCES

Arp, C., Bondurant, A., & Clement, S. (2024). *Winter open-water zone remote sensing (2017-2023) and field (2023) data from the Yukon and Kuskokwim rivers and their tributaries in western Alaska*. Arctic Data Center. https://doi.org/10.18739/A2086372J

Ashton, G. D. (2011). River and lake ice thickening, thinning, and snow ice formation. *Cold Regions Science and Technology*, *68*(1), 3–19. https://doi.org/10.1016/j.coldregions.2011.05.004

Belore, H. S., Burrell, B. C., & Beltaos, S. (1990). Ice jam mitigation. *Canadian Journal of Civil Engineering*, *17*(5), 675–685. https://doi.org/10.1139/l90-081

Beltaos, S., & Burrell, B. C. (2021). Effects of river-ice breakup on sediment transport and implications to stream environments: A review. *Water*, *13*(18), 2541.

Burrell, B. C., Beltaos, S., & Turcotte, B. (2021). Effects of climate change on river-ice processes and ice jams. *International Journal of River Basin Management*, *1-21*, 421–441. https://doi.org/10.1080/15715124.2021.2007936

Chikita, K. A., Kemnitz, R., & Kumai, R. (2002). Characteristics of sediment discharge in the subarctic Yukon River, Alaska. *Catena*, *48*(4), 235–253. https://doi.org/10.1016/S0341-8162(02)00032-2

Dornblaser, M. M., & Striegl, R. G. (2009). Suspended sediment and carbonate transport in the Yukon River Basin, Alaska: Fluxes and potential future responses to climate change. *Water Resources Research*, *45*(6), W06411. https://doi.org/10.1029/2008WR007546

Eidam, E. F., Langhorst, T., Goldstein, E. B., & McLean, M. (2022). Open-OBS: Open-source, low-cost optical backscatter sensors for water quality and sediment-transport research. *Limnology and Oceanography: Methods*, *20*(1), 46–59. https://doi.org/10.1002/lom3.10469

Engram, M., Meyer, F., Brown, D., Clement, S., Bondurant, A., Spellman, K., Oxtoby, L., & Arp, C. D. (2024). Detecting early winter open-water zones on Alaskan rivers using dual-polarized C-band Sentinel-1 synthetic aperture radar (SAR). *Remote Sensing of Environment*, *305*, 114096. https://doi.org/10.1016/j.rse.2024.114096

Ettema, R., & Daly, S. F. (2004). *Sediment transport under ice*. Engineer Research and Development Center Hanover NH Cold Regions Research and Engineering Lab.

Kalke, H., McFarlane, V., Schneck, C., & Loewen, M. (2017). The transport of sediments by released anchor ice. *Cold Regions Science and Technology*, *143*, 70–80. https://doi.org/10.1016/j.coldregions.2017.09.003

Kämäri, M., Alho, P., Veijalainen, N., Aaltonen, J., Huokuna, M., & Lotsari, E. (2015). River ice cover influence on sediment transportation at present and under projected hydroclimatic conditions. *Hydrological Processes*, *29*(22), 4738–4755. https://doi.org/10.1002/hyp.10522

Kempema, E. W., & Ettema, R. (2011). Anchor ice rafting: Observations from the Laramie River. *River Research and Applications*, *27*(9), 1126–1135. https://doi.org/10.1002/rra.1450

Kempema, E. W., Reimnitz, E., & Barnes, P. W. (2001). Anchor-ice formation and ice rafting in southwestern Lake Michigan, U.S.A. *Journal of*

Sedimentary Research, *71*(3), 346–354. https://doi.org/10.1306/2dc40948-0e47-11d7-8643000102c1865d

Knighton, D. (1998). *Fluvial forms and processes: A new perspective*. Oxford University Press Inc.

Langhorst, T., Pavelsky, T., Eidam, E., Cooper, L., Davis, J., Spellman, K., Clement, S., Arp, C., Bondurant, A., Friedman, E., & Gleason, C. (2023). Increased scale and accessibility of sediment transport research in rivers through practical, open-source turbidity and depth sensors. *Nature Water*, *1*, 760–768. https://doi.org/10.21203/rs.3.rs-2793579/v1

Lawson, D. E., Research, C. R., & Laboratory, E. (1986). *Morphology, hydraulics and sediment transport of an ice-covered river: Field techniques and initial data*. US Army Cold Regions Research and Engineering Laboratory.

Leopold, L. B., Wolman, M. G., & Miller, J. P. (1964). *Fluvial processes in geomorphology* (p. 522). Freeman.

Lyell, C. (1868). *Principles of geology*. New York.

Masterson, D. M. (2009). State of the art of ice bearing capacity and ice construction. *Cold Regions Science and Technology*, *58*(3), 99–112. https://doi.org/10.1016/j.coldregions.2009.04.002

McNamara, J. P., & Kane, D. L. (2009). The impact of a shrinking cryosphere on the form of arctic alluvial channels. *Hydrological Processes*, *23*, 159–168. https://doi.org/10.1002/hyp.7199

Osterkamp, T. E. (1977). Frazil-ice nucleation by mass-exchange processes at the air-water interface. *Journal of Glaciology*, *19*(81), 619–627. https://doi.org/10.3189/S0022143000215529

Osterkamp, T. E., & Gosink, J. P. (1983). Frazil ice formation and ice cover development in interior Alaska streams. *Cold Regions Science and Technology*, *8*(1), 43–56. https://doi.org/10.1016/0165-232X(83)90016-2

Reimnitz, E., Kempema, E. W., & Barnes, P. W. (1987). Anchor ice, seabed freezing, and sediment dynamics in shallow Arctic Seas. *Journal of Geophysical Research, Oceans*, *92*(C13), 14671–14678. https://doi.org/10.1029/JC092iC13p14671

Schneider, W., Brewster, K., & Kielland, K. (2015). Team building on dangerous ice: A study in collaborative learning. *Arctic*, *68*(3), 399–404.

Syvitski, J. P. M. (2002). Sediment discharge variability in Arctic rivers: Implications for a warmer future. *Polar Research*, *21*(2), 323–330. https://doi.org/10.1111/j.1751-8369.2002.tb00087.x

Syvitski, J. P. M., Vorosmarty, C. J., Kettner, A. J., & Green, P. (2005). Impact of humans on the flux of terrestrial sediment to the global coastal ocean. *Science*, *308*(15), 376–380.

Turcotte, B., Morse, B., Bergeron, N. E., & Roy, A. G. (2011). Sediment transport in ice-affected rivers. *Journal of Hydrology*, *409*(1), 561–577. https://doi.org/10.1016/j.jhydrol.2011.08.009

White, K. D., & Kay, R. L. (1997). Dusting procedures for advance ice-jam mitigation measures. *Journal of Cold Regions Engineering*, *11*(2), 130–145. https://doi.org/10.1061/(ASCE)0887-381X(1997)11:2(130)

Yang, X., Pavelsky, T. M., & Allen, G. H. (2020). The past and future of global river ice. *Nature*, *577*(7788), 69–73. https://doi.org/10.1038/s41586-019-1848-1

How to cite this article: Arp, C. D., Bondurant, A. C., Clement, S., Eidam, E., Langhorst, T., Pavelsky, T. M., Davis, J., & Spellman, K. V. (2024). Observation of high sediment concentrations entrained in jumble river ice. *River Research and Applications*, 1–11. https://doi.org/10.1002/rra.4309